

See discussions, stats, and author profiles for this publication at: <https://www.researchgate.net/publication/272364808>

Ionic conductivity and molecular dynamic behavior in supramolecular ionic networks; The effect of lithium salt addition

ARTICLE *in* ELECTROCHIMICA ACTA · JANUARY 2015

Impact Factor: 4.5 · DOI: 10.1016/j.electacta.2015.02.064

READS

59

6 AUTHORS, INCLUDING:



Haijin Zhu

Deakin University

36 PUBLICATIONS 220 CITATIONS

SEE PROFILE



Alexander S. Shaplov

Russian Academy of Sciences

61 PUBLICATIONS 1,081 CITATIONS

SEE PROFILE



David Mecerreyes

Universidad del País Vasco / Euskal Herriko...

199 PUBLICATIONS 5,873 CITATIONS

SEE PROFILE



Maria Forsyth

Deakin University

479 PUBLICATIONS 14,288 CITATIONS

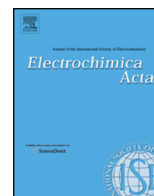
SEE PROFILE



Contents lists available at ScienceDirect

Electrochimica Acta

journal homepage: www.elsevier.com/locate/electacta



Ionic conductivity and molecular dynamic behavior in supramolecular ionic networks; the effect of lithium salt addition

M.Ali Aboudzadeh^a, Haijin Zhu^{b,*}, Cristina Pozo-Gonzalo^{b,*}, Alexander S. Shaplov^c, David Mecerreyes^a, Maria Forsyth^b

^a POLYMAT, University of the Basque Country UPV/EHU, Joxe Mari Korta Center, Avda. Tolosa 72, 20018 Donostia-San Sebastian, Spain

^b IFM, Deakin University, Burwood, VIC 3125, Australia

^c A.N Nesmeyanov Institute of Organoelement Compounds Russian Academy of Sciences (INEOS RAS), Vavilov str. 28, 119991, GSP-1, Moscow, Russia

ARTICLE INFO

Article history:

Received 21 November 2014

Received in revised form 4 February 2015

Accepted 7 February 2015

Available online xxx

Keywords:

Supramolecular materials

ionic liquids

ionic conductivity

lithium

solid-state NMR

ABSTRACT

Supramolecular ionic networks combine singular properties such as self-healing behaviour and ionic conductivity. In this work we present an insight into the ionic conductivity and molecular dynamic behaviour of an amorphous and semicrystalline supramolecular ionic networks (iNets) that were synthesised by self-assembly of difunctional imidazolium dicationic molecules coupled with (trifluoromethane-sulfonyl) imide dianionic molecules. Relatively low ionic conductivity values were obtained for the semicrystalline iNet below its melting point ($T_m = 101^\circ\text{C}$) in comparison with the amorphous iNet for which the conductivity significantly increased (~ 3 orders of magnitude) above 100°C . Upon LiTFSI doping, the semicrystalline iNet reached conductivity values $\sim 10^{-3} \text{ S cm}^{-1}$ due to enhanced mobility of the network which was supported by solid-state static NMR. Furthermore, the overlapping of ^{19}F and ^7Li resonance lines from both the semicrystalline network and the LiTFSI suggests fast molecular motions.

© 2015 Elsevier Ltd. All rights reserved.

1. Introduction

The recent strategies of self-assembly and supramolecular chemistry are opening new opportunities for the bottom-up design of functional materials [1–7]. For over a decade, functional supramolecular materials assembled via non-covalent interactions, such as hydrogen bonding, π – π stacking or metal–ligand bonds have been attracting a great deal of attention [8–10]. Among non-covalent interactions, ionic interactions are an attractive, unexplored and viable approach to the construction of supramolecular materials. The early history of ionic interactions in polymers dates back to the developments of polyelectrolytes and ionomers. Polyelectrolytes possess a high content of ionic groups that afford them properties such as ionic conductivity, enabling a variety of potential applications such as solid-state polymer electrolytes in Li-ion battery and fuel cells, and so on [11–13].

In the last years, new types of polyelectrolytes and ionic materials have been developed by introduction of new cations and anions that come from ionic liquid chemistry [14,15]. For instance,

the preparation of supramolecular ionic networks was reported by combining multi-cationic and multi-anionic compounds [16–19]. In this case, complex molecules such as alkyl phosphonium dications were employed together with multicarboxylate molecules. Recently, some of us reported examples of using simple acid–base ionic complexes for the generation of supramolecular ionic networks [20–23]. The materials were similar than protic ionic liquids where multifunctional carboxylic acids such as citric acid and diamines were combined. In these works, the resulting ionic networks demonstrated sharp changes in rheological and conductivity properties through a temperature range of 30 to 80°C . This fact suggested their potential use as self-healing materials as well as ion conducting materials [20]. However, the supramolecular ionic networks possessed some intrinsic issues, related to the constituent carboxylate compounds, such as water sensitivity, poor thermal stability and low ionic conductivity.

More recently, we developed a new family of supramolecular ionic networks (iNet) based on highly delocalized di-anionic monomers that exhibited good thermal and water stability. These iNets formed by the self-assembly of difunctional imidazolium dicationic molecules coupled with (trifluoromethane-sulfonyl) imide dianionic molecules presented superior transport properties and self-healing type rheological behaviour [24]. Although, most of the synthesized compounds were semicrystalline, amorphous networks were also obtained using aromatic asymmetric dianions.

* Corresponding authors. Tel.: +61392446634.

E-mail addresses: h.zhu@deakin.edu.au (H. Zhu), cpg@deakin.edu.au (C. Pozo-Gonzalo).

These amorphous ionic networks showed a significantly higher ionic conductivity than the semicrystalline iNets. Following that study, the goal of this article is to understand the relationship between morphology and ionic conductivity of an semicrystalline and amorphous ionic networks using temperature and time-sweep tests. The impact of addition of lithium salt on the transport properties, in particular conductivity, of the semicrystalline networks is evaluated for the first time. Thermal and molecular dynamics behaviour of the neat and lithium doped semicrystalline network was investigated by impedance spectroscopy, differential scanning calorimeter (DSC) and static solid-state NMR spectroscopy.

2. Experimental

2.1. Preparation of lithium doped supramolecular ionic network

Lithium bis(trifluoromethanesulfonyl) imide (LiTFSI) (Aldrich, 99%) was used as received. Supramolecular ionic networks **iNet-1** and **iNet-2** (Table 1) were synthesised by combining highly delocalised dianions with geminal di-imidazolium dications as the building blocks. These novel dianionic monomers were synthesised by the chemical modification of disulfonate sodium salts to highly delocalized anions (trifluoromethane-sulfonyl) imide. A more detailed synthesis has been reported in the previous study [24]

Doping was achieved by melting the supramolecular ionic network **iNet-1** with either 5 or 10 mol% LiTFSI in a high-purity argon environment glove box and stirring for 1 hour at 110 °C to ensure that the LiTFSI had completely dissolved.

2.2. Characterization

A Mettler Toledo differential scanning calorimeter (DSC) was used to investigate the thermal properties of the samples. Measurements were made from -70 °C to 180 °C at cooling and heating rates of 10 °C/min. Samples weighed were ~9–12 mg. Glass transition temperature (T_g) was determined automatically by the instrument from the second heating trace and reported as the midpoint of the thermal transition.

The ionic conductivities of all samples were measured using AC impedance spectroscopy on a Solartron potentiostat equipped with modulab MTS software. Samples were dried overnight inside a vacuum oven at 70 °C prior ionic conductivity characterisation.

For solid samples, pellets, 0.8–1.0 mm thick and ~13 mm diameter were prepared by pressing in a KBr die under 3 tons of load for 5 minutes. The prepared pellets were sandwiched between two circular stainless steel electrodes in hermetically sealed conductivity cells (Advanced Industrial Services, Moorabbin, Australia). Data were collected over a frequency range of

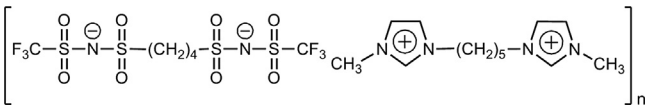
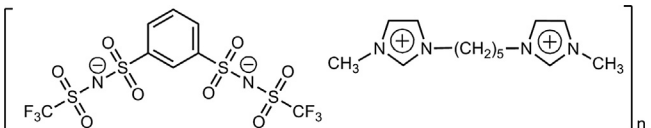
100 mHz–1 MHz and specific temperature range for each sample were considered, in heating and cooling cycles, at 5 °C intervals under single sine wave acquisition mode at 100 mV signal voltage amplitude and auto current mode. The cooling cycle was carried out immediately after, and at the same rate as the heating cycle. The temperature was controlled using a Eurotherm model 3504 temperature controller and a 28 V/32 W heater (Helios Electroheat Pty Ltd Cheltenham, Australia). For liquid samples, a homemade conductivity cell was used, consisting of two platinum electrodes immobilized in a resin and embedded into a glass matrix. Each of the wires was electrically connected to the potentiostat. The cell was dipped into a glass vial containing the liquid sample while ensuring complete immersion of the wires and avoiding bubbles. Water and air were excluded from the sample using rubber seal and teflon tape. Conductivity standard KCl solution (concentration: 0.01 mol/l, conductivity: 1.413 mS/cm at 25 °C) was used to calibrate this conductivity cell. An interval of 20 min was allowed between each measurement temperature (i.e., after each 5 or 10 °C step). Multiple measurements were carried out to check for stability and reproducibility in the Nyquist plots for each of the samples. Nyquist plots of the impedance data were used to determine the sample resistance from the intercept (or the first touch-down) of the real axis.

All the ^1H , ^7Li , and ^{19}F static solid-state NMR experiments were performed on a Bruker Avance III 300 wide bore NMR spectrometer operating at 300.13 MHz. A 4 mm double resonance Magic Angle Spinning (MAS) probe head was used to record the spectra from both the MAS and stationary powder samples. For both ^1H and ^{19}F NMR experiments, the 90° pulse lengths were 2.5 μs corresponding to rf-field strengths of 100 kHz, and the recycle delays were 20 s to allow the system to recover to equilibrium. The 90° pulse lengths for ^7Li were 4 μs corresponding to rf-field strengths of 62.5 kHz, and recycle delay was 5 s ($t_1\{^7\text{Li}\} < 1\text{ s}$). The sample temperatures for the variable temperature (VT) experiments were calibrated with lead nitrate, using the method described in the literature [25,26].

The static NMR measurements were performed by holding the temperature at 120 °C for 5 minutes before measurements to remove any thermal history, and then air-quenched to room temperature and equilibrated for approximately 10 min before NMR measurements. During NMR measurement, the temperature was increased from 20 °C to 70 °C, every 10 °C stepwise. Equilibration time of 5 min was allowed at each temperature before the measurements. Unless otherwise stated, the temperature procedures for all the following variable-temperature NMR experiments are the same.

The ^1H diffusion coefficients were measured with pulse-field gradient (PFG) NMR experiments on the same NMR spectrometer as the static NMR experiments, but equipped with a 5 mm diff50 pulse-field gradient probe. The samples were packed to a

Table 1
Supramolecular ionic networks iNets.

	iNet-1
	iNet-2

height of 50 mm in a 5 mm Schott E NMR tube in a nitrogen-filled glove box and sealed with Teflon tape and a cap. The ^1H NMR signals were used for the determination of the diffusion coefficient of the ionic polymer chains. The pulsed-field gradient stimulated echo (PFG-STE) pulse sequence [27] was used to obtain the diffusion coefficients of different species.

3. Results and discussion

3.1. Conductivity behaviour

Fig. 1 depicts the ionic conductivity as a function of temperature in both heating and cooling cycles for the neat semicrystalline network, **iNet-1**, and LiTFSI doped **iNet** (Fig. 1a), and amorphous network, **iNet-2** (Fig. 1b) (Table 1). The ionic conductivity of supramolecular ionic networks was measured by AC impedance spectroscopy.

iNet-2 presents higher values of ionic conductivity ($10^{-6} \sim 10^{-3} \text{ S cm}^{-1}$) throughout the entire temperature range (20–100 °C) in comparison with semicrystalline **iNet-1**. Also, the temperature dependence of the conductivity for neat **iNet-2** is close to linear behaviour at higher temperature values with no apparent conductivity hysteresis between heating and cooling cycling (Fig. 1b). On the other hand, at temperatures below 70 °C the semicrystalline neat **iNet-1** demonstrated close to Arrhenius behaviour with the conductivity increasing from 1.3×10^{-10} to $4.4 \times 10^{-9} \text{ S cm}^{-1}$ upon heating (Fig. 1a). Interestingly, at temperatures close to its melting point ($\sim 100^\circ\text{C}$), a sharp increase in ionic conductivity, \sim three orders of magnitude, was observed leading to a conductivity of $10^{-5} \text{ S cm}^{-1}$. In a similar way, during the cooling cycle a high conductivity was also attained for the melted **iNet-1** which decreased at temperature below its melting point. However, the material showed a hysteresis of more than 1 order of magnitude between the cooling and heating cycles which is believed to be directly related to the crystalline content of the sample.

The conductivity behaviour as a function of temperature for **iNet-1** upon addition of 5 mol% and 10 mol% LiTFSI is shown in Fig. 1a. It can be seen that, upon addition of Li salt, a significant enhancement in the conductivity of around 3 or 4 orders of magnitude is obtained compared to the neat sample leading to values close to $10^{-3} \text{ S cm}^{-1}$. As a complementary study, the ionic conductivity of neat **iNet-1** was investigated as a function of time

following a rapid quenched from the liquid state (115 °C) to room temperature using liquid nitrogen. For this sample, the impedance spectra were collected at times from 0.5–80 hours at intervals of 20 min. Furthermore, an equilibration time of 20 min was used to stabilize the temperature at RT before the beginning the next measurement. The conductivity for the quenched sample at room temperature over this time period was around $10^{-6} \text{ S cm}^{-1}$, whereas the unquenched sample achieved this value of conductivity at about 100 °C (Fig. 1a) which may be due to the formation of a metastable system.

3.2. Thermal analysis

The thermal behaviour of supramolecular ionic networks after doping with LiTFSI, was investigated by differential scanning calorimetry (DSC). The semicrystalline supramolecular ionic network neat and doped **iNet-1** showed a sharp melting point (T_m) in the first heating cycle, but only a glass transition temperature at lower temperatures in the second heating cycle (Fig. 2 a and b) which could be related to a reduction of the crystallinity of the network.

In contrast, amorphous **iNet-2** demonstrated only a glass transition at -20°C in subsequent heating cycles. The addition of LiTFSI (10 mol%) to the neat **iNet-1** caused a decrease in both melting point and glass transition temperature, $T_m(\text{neat}) = 101^\circ\text{C}$; $T_m(10 \text{ mol}\%) = 96^\circ\text{C}$; $T_g(\text{neat}) = -19^\circ\text{C}$; $T_g(10 \text{ mol}\%) = -23^\circ\text{C}$. The melting peak also broadened significantly and the ΔH slightly decreased ($\sim 3\%$) (Fig. 3). Both the reduced melting temperature, ΔH decrease and the broadening of the melting endotherm confirm that doping leads to a slight reduction of the crystallinity of the network. This is a well-known favourable condition for ionic conductivity enhancement, but the three order of magnitude enhancement cannot be justified but this small crystallinity decrease. For this reason, solid-state static NMR was carried out for better understanding.

3.3. Solid-state nuclear magnetic resonance spectroscopy

Fig. 3 compares the static ^1H and ^{19}F NMR spectra of the neat **iNet-1** and 10% LiTFSI doped **iNet-1** samples. The ^1H and ^{19}F static NMR spectra of solids usually show a broad and featureless peak resulting from the strong homonuclear dipole-dipole interactions. Since these interactions can be partially averaged by dynamics, the

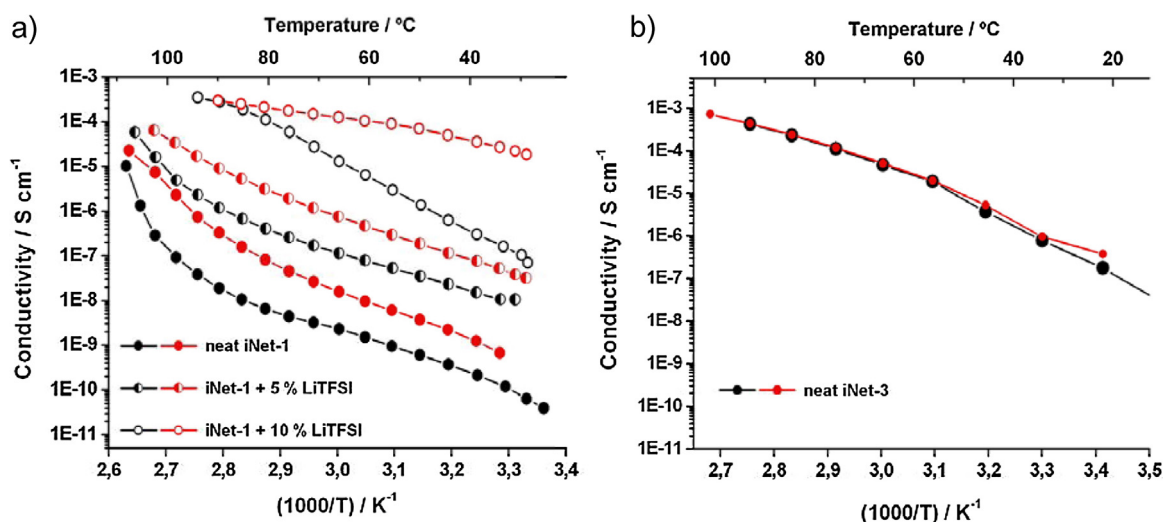


Fig. 1. Temperature dependence of ionic conductivity a) for neat **iNet-1** and doped **iNet-1** with 5 mol% and 10 mol% of LiTFSI, and b) for neat **iNet-2**. Heating and cooling cycles are shown in black and red colors, respectively. (For interpretation of the references to color in this figure legend, the reader is referred to the web version of this article.)

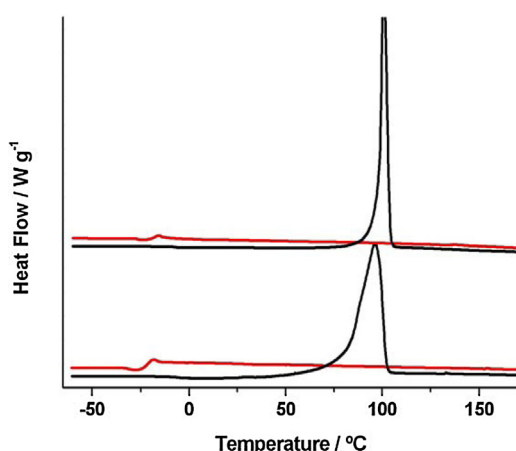


Fig. 2. DSC profile of neat **iNet-1** (upper) and after addition of 10 mol% LiTFSI (lower), first heating cycle (black) and second heating cycle (red). (For interpretation of the references to color in this figure legend, the reader is referred to the web version of this article.)

line widths of these spectra contain useful information about molecular motions and are therefore well suited for studies of local molecular dynamics. In the systems studied, ^1H is only present in the polymer matrix, while ^{19}F exists in both the polymer matrix and the doped LiTFSI. This feature allows us to analyse the motions of the polymer chain and the doped LiTFSI molecules separately. As expected, all ^1H and ^{19}F spectra show progressive line-narrowing with increasing temperature indicating increasing molecular dynamics. Comparing the ^1H and ^{19}F line widths between the neat **iNet-1** and 10% LiTFSI doped **iNet-1** samples, we note that the latter shows systematically narrower lines than those of the neat sample. This suggests that polymer chains are mobilized in the presence of LiTFSI, and this is consistent with the DSC results which show lower melting and glass transition temperature and broader melting endotherm upon the addition of LiTFSI. Also, at 70 degrees three peaks can be clearly identified in the ^1H spectrum of the doped sample. These peaks, from left (lower field) to right (higher field), are attributed to the protons in the aromatic rings, CH_2 groups and CH_3 groups, respectively.

Moreover, it is also noted that in the ^{19}F NMR spectra of the 10% LiTFSI doped **iNet-1** sample, the ^{19}F resonance lines from both the polymer and the LiTFSI overlapped and appear as a single narrow

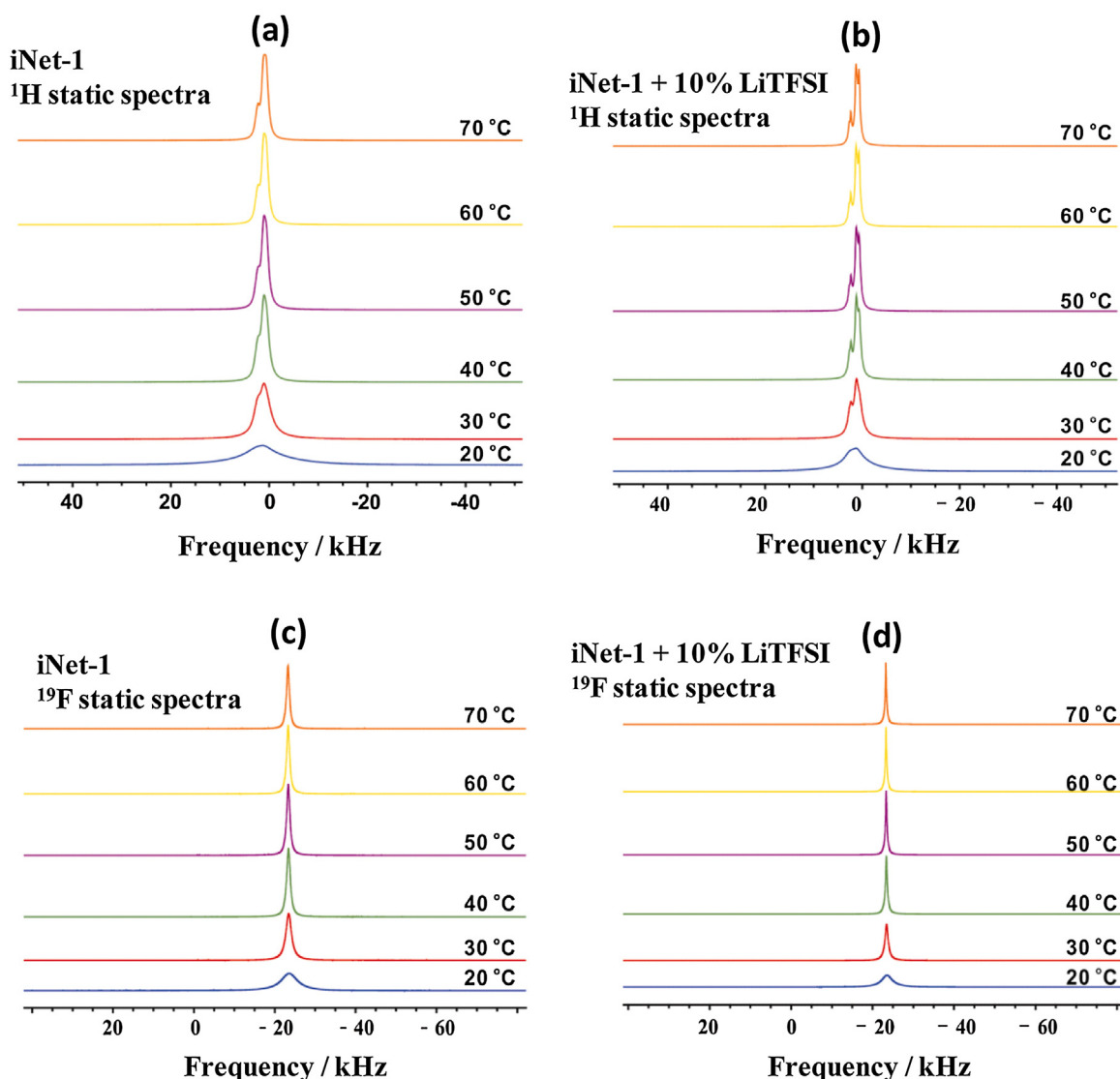


Fig. 3. Static ^1H and ^{19}F NMR spectra of the neat **iNet-1** (a and c, respectively) and after addition of 10 mol% LiTFSI (b and d, respectively).

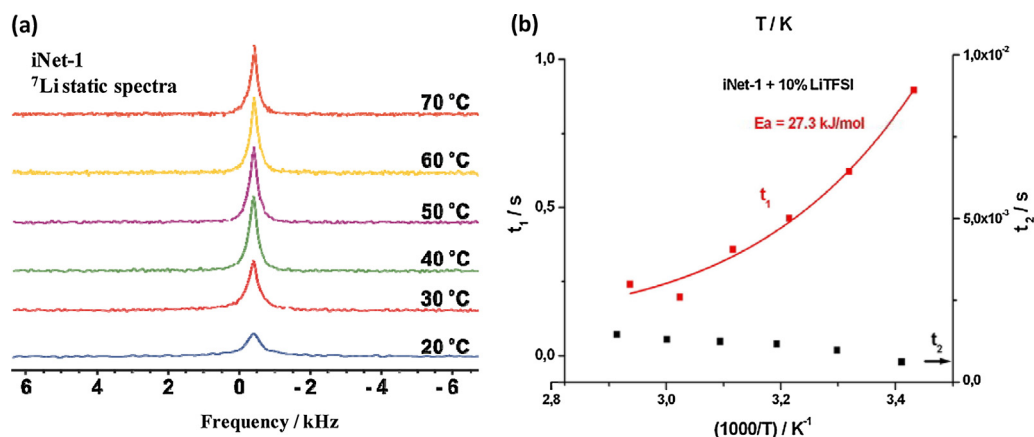


Fig. 4. a) Static ^7Li NMR spectra of the 10 mol% LiTFSI doped **iNet-1** and b) ^7Li T_1 and T_2 measured at different temperatures. The red line shows a BPP fit to the experimental T_1 data. (For interpretation of the references to color in this figure legend, the reader is referred to the web version of this article.)

line, indicating that both the polymer and the LiTFSI are undergoing fast molecular motions.

Fig. 4a shows the static ^7Li NMR spectra of the 10% LiTFSI doped **iNet-1** sample. The typical quadrupolar line shape for ^7Li in polymer electrolytes systems (i.e. broad-based line and superimposed narrow central line) is not observed in these spectra. This implies that fast lithium ion dynamics cause collapse of the broad satellite line into the central transition, and the increasing ion dynamics with increasing temperature lead to narrowing of the central transition line. At high temperatures, the motion of the lithium ions results in the ^7Li spectra becoming a single Lorentzian line with no apparent quadrupolar broadening. Assuming the lineshape is perfectly Lorentzian, the t_2 relaxation time can be estimated from the full width at half maximum (FWHM) using the equation $t_2 = 1/(\pi \cdot \text{FWHM})$. In order to understand the molecular motions near the Larmor frequency range, t_1 was measured at different temperatures using the saturation-recovery method. The obtained t_1 and t_2 for ^7Li are plotted against $1000/T$ (K^{-1}) in Fig. 4b. Assuming a single exponential correlation function and fitting the t_1 data with the BPP expression, the activation energy was estimated to be 27.3 kJ/mol. Apparently, in the studied temperature range of 293.2 K – 343.2 K, the lithium ion is in the slow-motion

range where the t_1 decreases and the t_2 increases with increasing temperature (molecular correlation time).

Fig. 5 shows the the proton diffusion coefficients of both neat **iNet-1** and 10% LiTFSI doped **iNet-1**. The 10% LiTFSI doped sample shows systematically higher diffusion coefficients than the neat sample at all temperatures studied. This means that with 10% LiTFSI doping, the translational motion of the polymer chains is increased. While this result is consistent with our previously showed static ^1H and ^{19}F NMR spectra, which show narrower lines (longer t_2) for the 10% LiTFSI doped **iNet-1** sample, it is obviously contrary to typical ionic liquid systems where the viscosity increases (hence diffusivity decreases) with the addition of the LiTFSI salt [28,29]. This phenomenon therefore suggests a synergistic effect between the supramolecular ionic network and the LiTFSI, and as a result both ions are mobilized. Combining the observations from the NMR relaxation and diffusion experiments, it can be concluded that both the rotational (or vibrational) motion and translational motions of the supramolecular ionic network are improved upon the addition of LiTFSI. ^7Li diffusion coefficients could not be obtained in this temperature range because of both short t_2 and slow apparent translational motions (i.e. low diffusivities) of ^7Li .

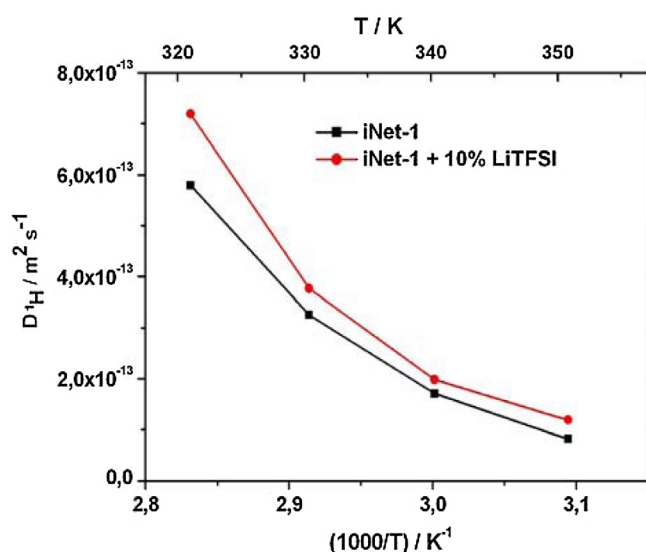


Fig. 5. Comparison of the ^1H diffusion coefficients at different temperatures for the neat **iNet-1** and 10% LiTFSI doped **iNet-1**.

4. Conclusion

Ionic conductivity of new semicrystalline and amorphous supramolecular ionic networks, **iNets**, has been investigated. Significant differences were observed in their transport properties depending on the crystalline state of the materials. The amorphous **iNets** showed relatively high ionic conductivity values ($10^{-6} \sim 10^{-3} \text{ S cm}^{-1}$) throughout the entire temperature range (20–100 °C) while the semicrystalline **iNets** showed relatively low values of ionic conductivity (1.3×10^{-10} to $4.4 \times 10^{-9} \text{ S cm}^{-1}$) at temperature below its melting. However, a sharp jump in conductivity (~ 3 orders of magnitude) was observed in the semicrystalline **iNets** upon melting. Furthermore, the effect of the addition of a lithium salt into the properties of the semicrystalline network was investigated in detail by impedance spectroscopy and NMR measurements. Upon doping the semicrystalline network with lithium bis(trifluoromethanesulfonyl) imide (LiTFSI), a significant enhancement in the conductivity, ~ 3 to 4 orders of magnitude, was obtained compared to the neat sample, and decreases in melting point and glass transition temperature were observed indicating a reduction on the crystallinity of the material. A detailed static solid-state NMR study of the doped sample

indicated that the **iNet** became more mobile in the presence of the lithium salt.

Supramolecular ionic networks showed intermediate ionic conductivity values between those of ionic liquids and polymer electrolytes. Furthermore, its ionic conductivity, as in the case of both ionic liquids and polymer electrolytes, strongly depended on the crystallinity and the doping of the materials.

Acknowledgements

Prof. Maria Forsyth wishes to acknowledge the financial support from the Australian Research Council (ARC) through the Australian Laureate program funding FL110100013. ARC is also acknowledged for funding Deakin University's Magnetic Resonance Facility through LIEF grant LE110100141. DM acknowledges the European Research Council for grant iPES ERC-Stg- 2012-306250. Assoc. Prof. Alexander S. Shaplov is grateful to the Russian Foundation for Basic Research for the financial support through projects no. 13-03-00343-a and 14-29-0403914_ofi_m. Finally authors would like to thank the European Commission for the International Research Staff Exchange Scheme (FP7-PEOPLE-2012-IRSES, project no. 318873 «IONRUN»).

References

- [1] J.M. Lehn, *Supramolecular Chemistry*, VCH Press, New York, 1995.
- [2] S.I. Stupp, V. LeBonheur, K. Walker, L.S. Li, K.E. Huggins, M. Keser, A. Amstutz, *Science* 276 (1997) 384.
- [3] J.F. Hulvat, S.I. Stupp, *Angew. Chem. Int. Ed.* 42 (2003) 778.
- [4] M. Yoshio, T. Mukai, H. Ohno, T. Kato, *J. Am. Chem. Soc.* 126 (2004) 994.
- [5] A. Schenning, A.F.M. Kilbinger, F. Biscarini, M. Cavallini, H.J. Cooper, P.J. Derrick, W.J. Feast, R. Lazzaroni, P. Leclere, L.A. McDonnell, E.W. Meijer, S.C.J. Meskers, *J. Am. Chem. Soc.* 124 (2002) 1269.
- [6] J.P. Hill, W. Jin, A. Kosaka, T. Fukushima, H. Ichihara, T. Shimomura, K. Ito, T. Hashizume, N. Ishii, T. Aida, *Science* 304 (2004) 1481.
- [7] P. Samori, V. Francke, K. Mullen, J.P. Rabe, *Chem. -Eur. J.* 5 (1999) 2312.
- [8] A. Ajayaghosh, S.J. George, *J. Am. Chem. Soc.* 123 (2001) 5148.
- [9] S.S. Babu, S. Prasanthkumar, A. Ajayaghosh, *Angew. Chem. Int. Ed.* 51 (2012) 1766.
- [10] Y. Yamamoto, T. Fukushima, W. Jin, A. Kosaka, T. Hara, T. Nakamura, A. Saeki, S. Seki, S. Tagawa, T. Aida, *Adv. Mater.* 18 (2006) 1297.
- [11] J.L. Lutkenhaus, P.T. Hammond, *Soft Matter* 3 (2007) 804.
- [12] W.H. Meyer, *Adv. Mater.* 10 (1998) 439.
- [13] B. Philipp, H. Dautzenberg, K.J. Linow, J. Koetz, W. Dawydoff, *Prog. Polym. Sci.* 14 (1989) 91.
- [14] D. Mecerreyes, *Prog. Polym. Sci.* 36 (2011) 1629.
- [15] J. Yian, D. Mecerreyes, M. Antonietti, *Prog. Polym. Sci.* 38 (2013) 1009.
- [16] M. Wathier, M.W. Grinstaff, *J. Am. Chem. Soc.* 130 (2008) 9648.
- [17] M. Wathier, M.W. Grinstaff, *Macromolecules* 43 (2010) 9529.
- [18] G. Godeau, L. Navailles, F. Nallet, X. Lin, T.J. McIntosh, M.W. Grinstaff, *Macromolecules* 45 (2012) 2509–2513.
- [19] X. Lin, M.W. Grinstaff, *Isr. J. Chem.* 53 (2013) 498.
- [20] M.A. Aboudzadeh, M.E. Muñoz, A. Santamaría, R. Marcilla, D. Mecerreyes, *Macromol. Rapid Commun.* 33 (2012) 314.
- [21] M.A. Aboudzadeh, M.E. Muñoz, A. Santamaría, M.J. Fernández- Berridi, L. Irusta, D. Mecerreyes, *Macromolecules* 45 (2012) 7599.
- [22] M.A. Aboudzadeh, M.E. Muñoz, A. Santamaría, D. Mecerreyes, *RSC Adv.* 3 (2013) 8677.
- [23] M.A. Aboudzadeh, M. Fernandez, M.E. Muñoz, A. Santamaría, D. Mecerreyes, *Macromol. Rapid. Commun.* 35 (2014) 460.
- [24] M. A. Aboudzadeh, A. S. Shaplov, G., Hernandez, P. S. Vlasov, E. I. Lozinskaya, C. Pozo-Gonzalo, M., Forsyth, Y. S. Vygodskib, D., Mecerreyes, 3 (2015) 2338.
- [25] X. Guan, R.E. Stark, *Solid State Nucl. Magn. Reson.* 38 (2010) 74.
- [26] A. Bielecki, D.P. Burum, *J. Magn. Reson. Ser.* 116 (1995) 215.
- [27] R.M. Corns, M.J.R. Hoch, T. Sun, J.T. Markert, *J. Magn. Reson.* 83 (1989) 252.
- [28] T. Wu, L. Hao, P. Chen, J.W. Liao, *Int. J. Electrochem. Sci.* 8 (2013) 2606.
- [29] H. Yoon, H. Zhu, A. Hervault, M. Armand, D.R. MacFarlane, M. Forsyth, *Phys. Chem. Chem. Phys.* 16 (2014) 12350.